

LIQUEFACTION POTENTIAL OF SABARMATI-RIVER SAND

S.V. Dinesh*, G. Mahesh Kumar*, Muttana S. Balreddy* and B.C. Swamy**

*Department of Civil Engineering

Siddaganga Institute of Technology, Tumkur-572103

**Department of Civil Engineering

Central Connecticut State University, New Britain, CT 06053, U.S.A.

ABSTRACT

Liquefaction of saturated sandy soils has been studied by several researchers and liquefaction potential depends on initial confining pressure, relative density, amplitude of cyclic stress, etc. The Bhuj earthquake caused extensive damage in several parts of Gujarat. In the present paper, the results of stress-controlled cyclic triaxial tests on soil samples obtained from the Sabarmati river-bed in the Ahmedabad city, Gujarat are reported for various relative densities at the 100-kPa confining pressure. The results of cyclic strength, excess pore water pressure development and dynamic properties are analyzed. The liquefaction resistance is qualitatively compared to that of the Toyoura sand. It is found that liquefaction strength increases with relative density and correlates well with the normalized shear strength obtained from the consolidated undrained tests.

KEYWORDS: Liquefaction, Pore Pressure Ratio, Cyclic Resistance Ratio, Shear Modulus

INTRODUCTION

Liquefaction is a phenomenon that leads to the complete loss of shear strength due to the development of excess pore water pressure. During the earthquakes, saturated sandy deposits undergo liquefaction. Generally, there will be a complete loss of strength or development of excessive strains. Liquefaction gained importance after the Niigata and Alaska earthquakes of 1964. There has been a lot of research in these years, and significant contributions have been made and state-of-the-art papers have been published to understand the concept (Lee and Seed, 1967; Ishihara et al., 1975; Ishihara, 1985; Li et al., 1988; Ishihara, 1993; Hyodo et al., 1998; Polito and Martin II, 2001; Baxter et al., 2008).

The liquefaction resistance is generally evaluated either by laboratory or field methods. In the laboratory method cyclic triaxial and simple shear tests are widely used on reconstituted or undisturbed soil samples. Liquefaction is a strain-softening type of undrained response involving excessive deformations. The liquefaction or cyclic softening is defined in terms of cyclic stress ratio to produce 5% double-amplitude axial strain or 100% excess pore water pressure development (i.e., zero deviator stress) in 20 cycles of uniform load application. This cyclic stress ratio is also called as cyclic resistance ratio (CRR), synonymous with the 'cyclic strength'.

In view of the difficulty in obtaining undisturbed soil samples, the liquefaction strength is obtained by using reconstituted soil samples. The liquefaction resistance of saturated reconstituted sands in laboratory has been studied extensively by several researchers (Seed, 1979; Finn, 1981; Govindaraju, 2005; Ravishankar, 2006), and it has been concluded that initial confining stress, cyclic shear stress and void ratio affect the liquefaction resistance. Tatsuoka et al. (1986) have shown for the Toyoura sand that CRR increases linearly with relative density up to 70%, and thereafter, CRR increases rapidly with an increase in relative density.

The Bhuj earthquake in 2001 caused extensive loss of life and damage to the infrastructure in Gujarat, India. There were wide-spread sand boils and liquefaction. Bhandari and Sharma (2001) have observed a pattern of damage in the Ahmedabad city, in which a number of damaged multistoried buildings were scattered on the left and right banks of the Sabarmati river. The damage was more around the Sabarmati river-bed, which consists of unconsolidated sediments of recent origin. In this connection, it has been felt necessary to establish liquefaction criteria for the unconsolidated sediments of the Sabarmati river-bed. Stress-controlled cyclic triaxial tests are conducted on sand sediments obtained from the Sabarmati river-bed and an attempt is made to qualitatively compare the current results with those of the Japanese Toyoura sand.

MATERIALS AND EXPERIMENTAL METHODS

1. Physical Properties of Materials

In the present investigation sand samples are obtained from the Sabarmati river-bed in the Ahmedabad city for characterizing the liquefaction potential. The sand samples are collected from a depth of 3 m from the excavated pits close to the Sabarmati river-bed. In the top 3 m the average SPT is found to be less than 10. In addition to being close to the river-bed it is likely that the top soil might have experienced cyclic softening or partial liquefaction.

Figure 1 shows the grain size distribution curves proposed by Iwasaki (1986) for the liquefaction-susceptible soils and the curves for the Sabarmati-river and Toyoura sands. It is observed that the grain size curves of both types of sands lie within the boundaries of most liquefiable soils. The grain size analysis of the Sabarmati-river sand indicates 91% sand and 9% non-plastic silt. The specific gravity is 2.63, and the maximum and minimum void ratios are 0.65 and 0.35, respectively. The coefficient of uniformity is 4.71 and the coefficient of curvature of the soil is 0.66. The soil is poorly graded sand containing silty fines and has the group symbol SP-SM. The maximum and minimum void ratios of the soil are measured by using the Japanese standard test method (JSA, 2009). In this method, the sand is placed in a cylindrical mould of 60-mm diameter and 40-mm height. The maximum void ratio is determined by pouring the sand through a funnel with 30° angle and 12-mm diameter outlet. The base of the funnel is kept close to the sand surface at all times, as the sand is evenly distributed across the surface. In the case of the minimum void ratio a 20 mm extension piece is added to the mould and the sand is placed in ten layers of 6 mm thickness each. Each layer is tamped manually with 20 blows (such that there are 5 blows on each side) with the amplitude of 50 mm by using a wooden mallet till the required density is achieved. The extension piece is then removed and the sand is levelled by using a straight edge. The results are compared with those of the vibratory table method as per the specifications of IS 2720, Part 14 (BIS, 2006), which are similar to the specifications of ASTM D 4253 (ASTM, 2006a) and ASTM D 4254 (ASTM, 2006b), and there is a very good correlation of the void ratios in both loose and dense states. The CRR of the Sabarmati-river sand is qualitatively compared with that of the Toyoura sand (Tatsuoka et al., 1986). The Toyoura sand has a specific gravity of 2.635, the maximum and minimum void ratios are 0.973 and 0.635, respectively, and D_{50} is 0.21 mm. The grain size analysis data of the Toyoura sand indicates 100% sand. Further, the coefficient of uniformity is 1.533, the coefficient of curvature of the soil is 1.046, and the sand is poorly graded with the group symbol SP. A powerful microscope is used to capture the image of the sand particles. The microscopic view and the morphological analysis (not reported here) indicate that the Sabarmati-river sand particles are subrounded in nature when compared to the Toyoura sand particles.

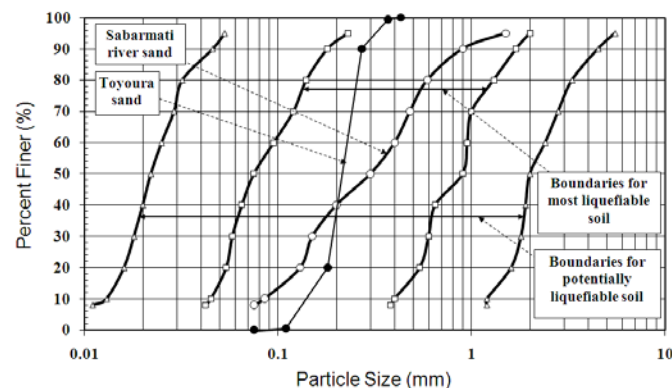


Fig. 1 Grain size distribution curves for liquefaction-susceptible soils, and Sabarmati-river and Toyoura sands (modified after Iwasaki, 1986)

2. Sample Preparation

Triaxial specimens of 50-mm diameter and 100-mm height are prepared by the dry deposition method. This method is adopted as it is not possible for obtaining looser specimens by the other methods (Wood et al., 2008). Wood et al. (2008) have also reported that there are some differences in the undrained response of the silty sand specimens of medium density, but there is no significant variation in

the undrained response of the specimens at higher density due to different depositional methods. Therefore, in order to have a uniform response, the dry deposition method is adopted to prepare the specimens of loose to dense state in the present investigation. In this method the specimen is prepared by placing the spout of the funnel at the bottom of the mould, and then the sand is poured into the funnel. The specimens are prepared in ten layers of equal thickness. In each layer a known mass of sand is poured gently through a sand pouring spout with zero height of fall, so that the sand gets deposited at low energy. To achieve higher densities, constant energy is applied on the sides of the mould for all layers by a wooden mallet. Each layer is tamped manually with 4 blows per layer (such that there is one blow on each side) with the amplitude of 50 mm so as to achieve the desired density. More blows are provided symmetrically to achieve higher densities. The sample is subjected to a small vacuum, and CO₂ gas is passed. Later, de-aired distilled water is circulated through the soil sample. Initially, the samples are subjected to a cell pressure of 100 kPa and a back pressure of 90 kPa, so that the effective confining pressure is 10 kPa, and this condition is maintained till the Skempton's pore pressure coefficient B exceeds 0.96. Then, the specimens are isotropically consolidated at an effective confining pressure of 100 kPa, and the consolidation process is continued till the end of the Casagrande's primary consolidation time. The reduction in the void ratio before and after consolidation is found to be in the range of 0.006 to 0.008. The samples are prepared at the relative densities of 45%, 55%, 62%, 69%, 77% and 85% (the initial relative densities are 43.33%, 53.00%, 59.66%, 65.67%, 75.33% and 83.33%; after consolidation, the samples have the relative densities of 44.67%, 55.33%, 62.06%, 68.96%, 77.18% and 84.75%, which are rounded off to 45%, 55%, 62%, 69%, 77% and 85%, respectively).

3. Stress-Controlled Tests

The testing is performed by using a cyclic triaxial shear test apparatus. The loading system in the apparatus consists of a servo-controlled hydraulic actuator. The amplitude and frequency of the load and waveform are controlled by a function generator. The data is obtained by a computer-controlled data acquisition system. The axial deformation of the soil sample is measured by the LVDTs of ± 10 mm range located outside the cell. The load is measured by a submersible load cell of 5 kN capacity located inside the cell. Further, there are 64 data points per load cycle.

The stress-controlled cyclic triaxial tests are performed under the undrained conditions. A sinusoidal load is applied by a double-acting, equal-area, hydraulic actuator with a total stroke of 100 mm. The actuator carries a state-of-the-art servo valve and the nitrogen-filled accumulators. The tests are carried out at a frequency of 0.1 Hz. This is less than the frequencies generally observed in the earthquake ground motions, but it has been shown that the liquefaction of sand is not frequency dependent (Wong et al., 1975; Wang and Kavazanjian Jr., 1989) and depends instead on the number and amplitude of the cycles of loading, etc. The tests are continued till the sample liquefies, which is characterized by the development of 100% excess pore water pressure ratio or 5% double-amplitude axial strain. After the completion of tests, the specimens are removed carefully from the triaxial cell, such that no particle is lost. Those are then dried and weighed for further calculations.

UNDRAINED CYCLIC BEHAVIOR

1. Experimental Programme

Table 1 shows the details of the program of cyclic tests. A total of 27 cyclic triaxial tests are carried out.

Table 1: Details of Experimental Program

S. No.	Relative Density (%)	Confining Pressure (kPa)	Frequency (Hz)	Cyclic Stress Ratio (CSR)
1	45	100	0.1	0.12, 0.15, 0.18 and 0.184
2	55	100	0.1	0.12, 0.15, 0.17, 0.19 and 0.20
3	62	100	0.1	0.12, 0.14, 0.18, 0.21 and 0.229
4	69	100	0.1	0.14, 0.17, 0.20 and 0.21
5	77	100	0.1	0.18, 0.20, 0.22 and 0.30
6	85	100	0.1	0.19, 0.20, 0.25, 0.30 and 0.33

2. Results and Discussion

2.1 Cyclic Strength

Figure 2(a) shows the deviator stress versus the number of cycles, Figure 2(b) shows the double-amplitude axial strain versus the number of cycles, and Figure 2(c) shows the excess pore water pressure ratio versus the number of cycles, on a sample at $D_r = 55\%$, at 100 kPa confining pressure, and on being subjected to the CSR value of 0.2. The deviator stress is constant on the compression and extension sides. After the third cycle, it is observed that the axial strain increases rapidly and the sample liquefies. The magnitude of double-amplitude strain is very low in the initial stages, and beyond the 0.5% strain level, the double-amplitude strain increases very rapidly. This strain level forms a threshold strain, beyond which there is a faster growth of the strain (or deformation) with cycles. The sample fails at the 5th cycle when the excess pore water pressure becomes equal to the applied confining pressure. At the conditions close to liquefaction, the double-amplitude axial strain is observed to be less than 5%. This may be considered as indicative of the initial liquefaction.

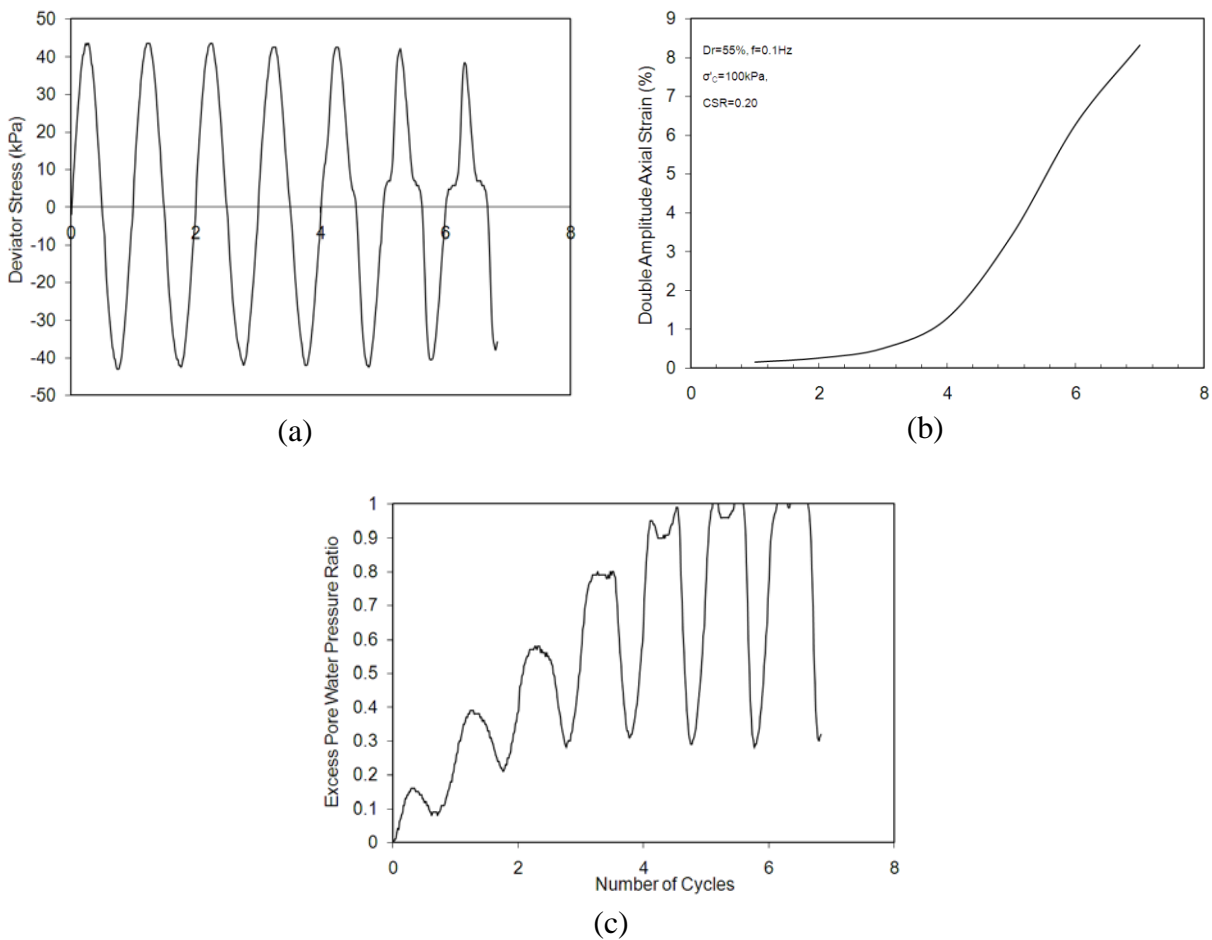


Fig. 2 Cyclic triaxial test results of Sabarmati-river sand sample at loose state having $D_r = 55\%$: a) deviator stress versus number of cycles; (b) double-amplitude axial strain versus number of cycles; (c) excess pore water pressure ratio versus number of cycles

Figure 3(a) shows the deviator stress versus the number of cycles, Figure 3(b) shows the double-amplitude axial strain versus the number of cycles, and Figure 3(c) shows the excess pore water pressure ratio versus the number of cycles, on a sample at $D_r = 85\%$, at 100 kPa confining pressure, and on being subjected to the CSR value of 0.2. The deviator stress is constant on the compression and extension sides. Beyond five cycles, it is observed that the axial strain increases rapidly and the sample liquefies. The magnitude of double-amplitude strain is very low in the initial stages, and beyond the 0.5% strain level, the double-amplitude strain increases rapidly. This strain level forms a threshold strain, beyond which there is a faster growth of the strain (or deformation) with cycles. The sample fails at the 16th cycle, when

the excess pore water pressure becomes equal to the applied confining pressure. At the conditions close to liquefaction, the double-amplitude axial strain is observed to be less than 5% and the sample fails due to the initial liquefaction. The dense sample shows the dilative tendency, as observed by the downward spikes in the pore pressure plot, and this is indicative of the limited potential for large deformations after the initial liquefaction (Baxter et al., 2008).

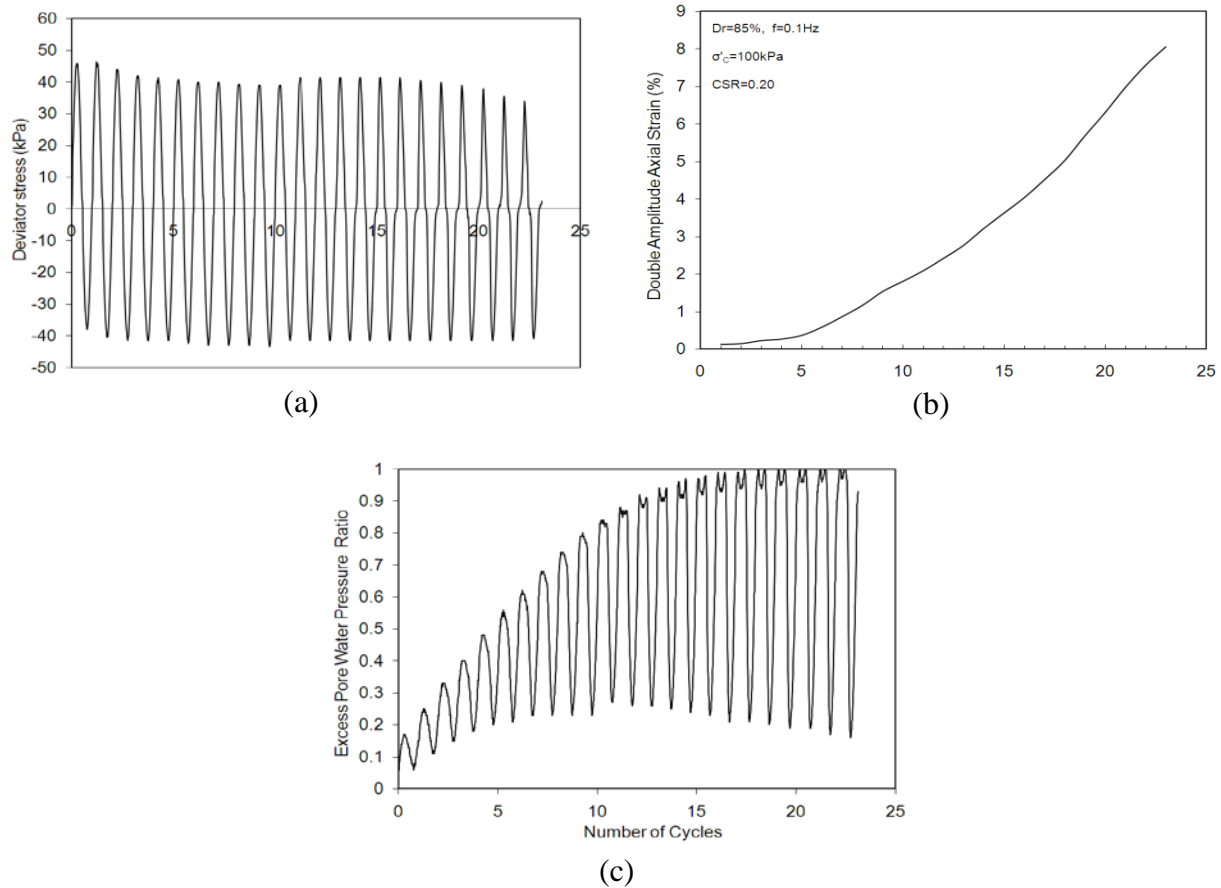


Fig. 3 Cyclic triaxial test results of Sabarmati-river sand sample at dense state having $D_r = 85\%$: a) deviator stress versus number of cycles; b) double-amplitude axial strain versus number of cycles; c) excess pore water pressure ratio versus number of cycles

Figure 4 shows the CSR curves for all the relative densities considered in the present investigation. The cyclic strength of sand is specified in terms of the magnitude of CSR required to produce 5% double-amplitude axial strain in the 20 cycles of uniform load application (as described by Ishihara, 1993) and is described as cyclic resistance ratio (CRR). The CRRs are 0.145, 0.16, 0.173, 0.19, 0.225, and 0.296 for the soil samples at the relative densities of 45%, 55%, 62%, 69%, 77%, and 85%, respectively. It is evident from the plot in Figure 4 that the cyclic strength of sand increases as the relative density increases. At low relative densities (i.e., 45% and 55%), the increase in CRR is low, when compared to the increase at higher relative densities (i.e., 77% and 85%).

Figure 5 shows CRR versus relative density curves for the Sabarmati-river and Toyoura sands (Tatsuoka et al., 1986). The Toyoura sand has $e_{max} = 0$, $e_{min} = 0$, and $G = 2$. It is observed that up to a relative density of 70%, CRR tends to increase linearly with an increase in the relative density, but for relative densities greater than 70%, CRR increases at a faster rate. The Sabarmati-river sand shows higher CRRs than the Toyoura sand. Further, the cyclic strength trends for both sands are qualitatively comparable. This clearly brings out the predominant effect of densification on the improvement in cyclic strength.

Figure 6 shows the threshold double-amplitude strain versus the number of cycles curves for various relative densities. The threshold double-amplitude strain is the strain beyond which the deformation increases rapidly. It is observed that when the relative density is higher, this strain is more. In most of the

cases the lower limit of this strain for different stress amplitudes is around 0.5% and above. This implies that when the threshold double-amplitude axial strain is less than 0.5%, the pore pressure build-up will be slow and the sample may not liquefy.

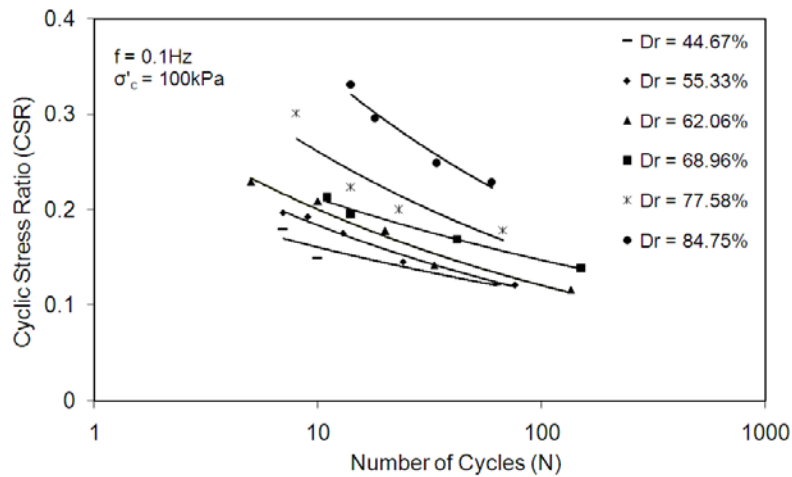


Fig. 4 CSR versus number of cycles curves for various relative densities

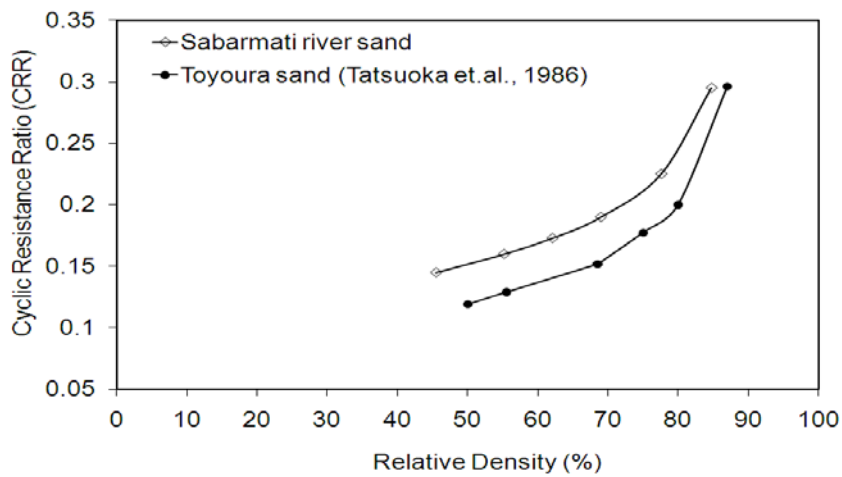


Fig. 5 CRR versus relative density curves for the Sabarmati-river and Toyoura sands

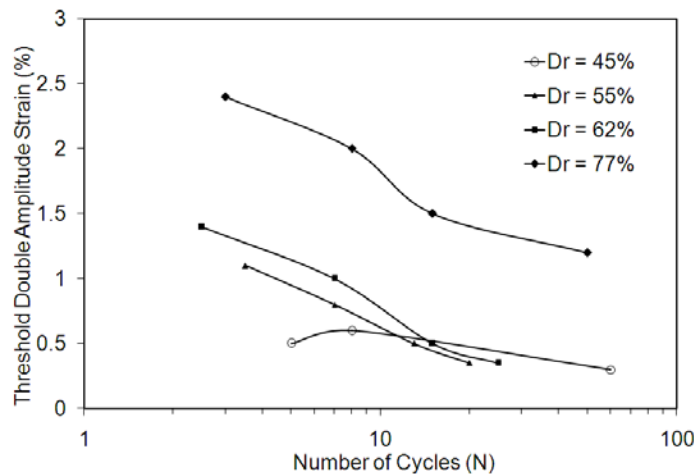


Fig. 6 Threshold double-amplitude strain versus number of cycles curves for various relative densities

Figure 7 shows the comparison of monotonic and cyclic stress paths at the relative density of 62%, corresponding to the void ratio of 0.464, at the 100 kPa confining pressure. The variation of double-amplitude axial strain is also indicated in the same plot. It is observed that when the cyclic stress path is close to the phase transformation line (after the 2nd cycle), the sample deforms rapidly.

Figure 8 shows the deviator stress and excess pore water pressure versus axial strain plots under the monotonic conditions for various relative densities, as obtained from the CU tests. The samples are prepared at the relative densities of 61.67%, 68%, 77% and 84% (after consolidation, the samples have the relative densities of 62.06%, 68.96%, 77.48% and 84.75%, which are rounded off to 62%, 69%, 77% and 85%, respectively). These results indicate that the peak deviator stress increases with an increase in the relative density. All samples with the relative densities greater than 69% show dilation. Therefore, the samples at higher relative densities (i.e., > 70%) show increased negative pore pressures due to the dilation resulting in an increase in the shear strength. For these dilative samples the pore pressure initially increases because of the compressive tendency and then decreases due to the shear. As this continues to decrease further it leads to a negative excess pore water pressure. As a result, the deviator stress increases and attains a peak value. The build-up of negative pore pressures in the samples at high relative densities indicates the possibility of the occurrence of cavitations (Brandon et al., 2006). If there are cavitations, there will be much scatter in the results, when the failure criterion is based on the peak deviator stress. When $\Delta U = 0$ is used as the failure criterion, there will be consistency in the undrained shear strength (Brandon et al., 2006). Therefore, in the present case, the criteria for the peak deviator stress and deviator stress at the critical state (at which the condition of zero pore pressure increment is used) are adopted to obtain the shear strength. Though the peak pore pressure and phase transformation strength criteria are considered for the correlation with CRR, there is much scatter in the results.

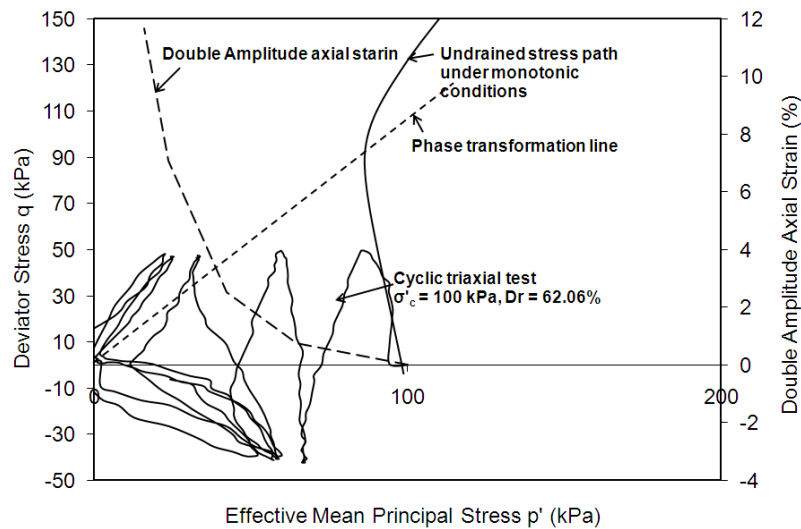


Fig. 7 Comparison of monotonic and cyclic stress paths

Figure 9 shows the CRR versus normalized shear strength plot, as obtained from the monotonic consolidated undrained (CU) tests, where normalized shear strength is the ratio of deviator stress (at the peak or critical state) to twice the effective confining pressure. An excellent correlation is observed between CRR and the normalized shear strength corresponding to the peak or critical state conditions in the CU tests. CRR can be obtained from the monotonic strength by using the following relations:

$$\frac{\sigma_d}{2\sigma'_c} = 0.097 + 0.018 \left(\frac{q_p}{2\sigma'_c} \right) \tag{1}$$

$$\frac{\sigma_d}{2\sigma'_c} = 0.043 + 0.0321 \left(\frac{q_c}{2\sigma'_c} \right) \tag{2}$$

where q_p is the peak deviator stress (in kPa) and q_c is the deviator stress (in kPa) at the critical state, under the monotonic conditions. The results based on the critical state failure criterion are observed to be better than those for the peak deviator stress criterion for the dilative conditions. Equation (1) can be used

for the normally consolidated conditions and Equation (2) is useful for both the normal consolidation and dilative conditions. Further, the undrained strength is equal to the drained strength at the critical state, and Equation (2) provides consistent values of CRR based on the drained and undrained strengths.

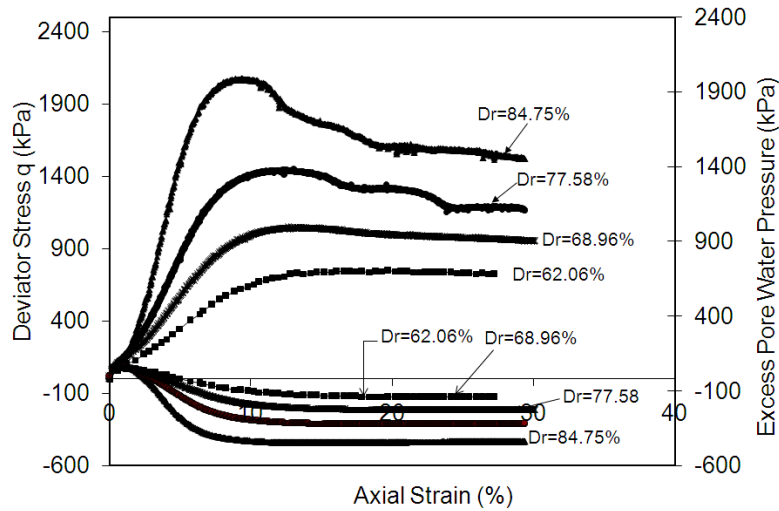


Fig. 8 Deviator stress and excess pore water pressure versus axial strain curves for various relative densities

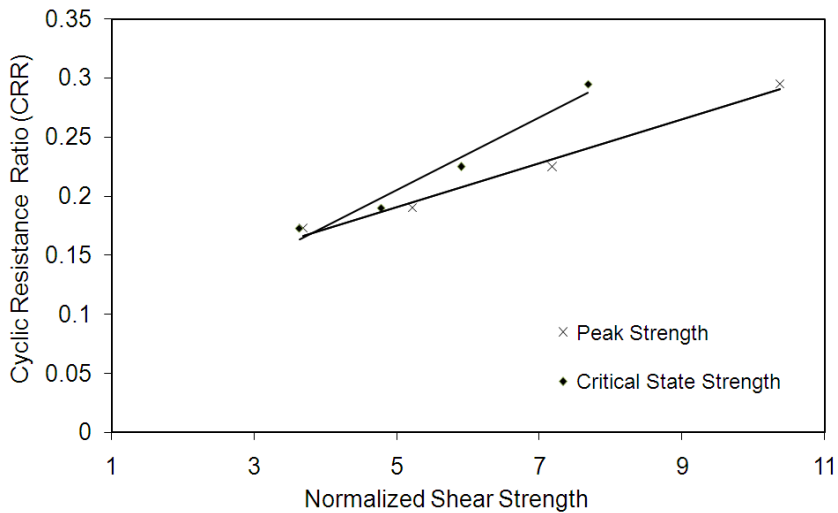


Fig. 9 CRR versus normalized shear strength curves from CU tests

2.2 Pore Pressure Development

Figure 10 shows the residual pore pressure ratio versus cycle ratio (i.e., N/NL) plot for the loose (with the relative density of 45%) and dense (with the relative density of 85%) states with nearly the same CSR values. In addition, the band of pore pressure ratio for all the relative densities and stress ratios in the present investigation is shown along with the data of Lee and Albaisa (1974). The pore pressure ratio is computed based on the residual pore water pressure at zero deviator stress at the end of each loading cycle. It is observed that the pore pressure ratio for the dense sample is more than that for the loose sample at any given cycle ratio till the cycle ratio of 0.55 (corresponding to the compression phase). Beyond this, the loose sample shows a faster build up due to continued compression, whereas the dense sample shows a slow build-up, when compared to the loose sample, due to dilation. The pore pressure band is obtained from 27 tests for a wide range of relative densities from 45% (for the loose state) to 85% (for the dense state). It may be observed that for any given cycle ratio, the pore pressure ratio of the Sabarmati-river sand is more than that reported by Lee and Albaisa (1974).

2.3 Dynamic Properties

Figure 11 shows the shear modulus versus single-amplitude axial strain data points for all the relative densities (from 45% to 85%). The shear modulus is computed here by using the Young’s modulus, where the Young’s modulus is a secant modulus obtained from the experimental data connecting the extreme points of the hysteresis loop. The shear modulus is strain dependent and it decreases with an increase in the axial strain. At low strains (i.e., less than 0.1%), shear moduli appear to increase with an increase in the relative density, but all the moduli are in a narrow band. If the shear modulus is captured at a very low strain, i.e., $\ll 0.01\%$, clear trends can be observed. However, the cyclic triaxial test being a large-strain test facility, the low-strain data cannot be obtained. At large strains, the shear modulus degradation is observed to be independent of the relative density. By about 1% axial strain, the degradation is complete, thus indicating a lower value of the shear modulus. Under the cyclic loading, growth in anisotropy is observed with the reversal of loading. This is reflected in the loss of contacts. This loss of contacts keeps increasing with the reversal of loading, and the effect of density is erased continuously. At large strains, say 1% and above, the system becomes unstable and the sample has the tendency to collapse, as the stiffness decreases due to the growth of anisotropy and the sample is no longer able to withstand the deviator stress. This behaviour has also been captured by the DEM simulations as in Dinesh (2002).

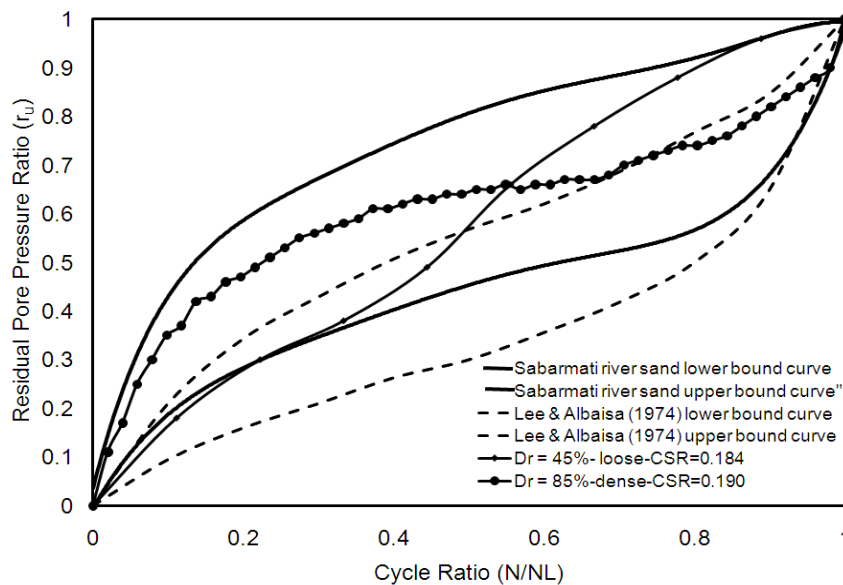


Fig. 10 Residual pore pressure ratio versus cycle ratio curves

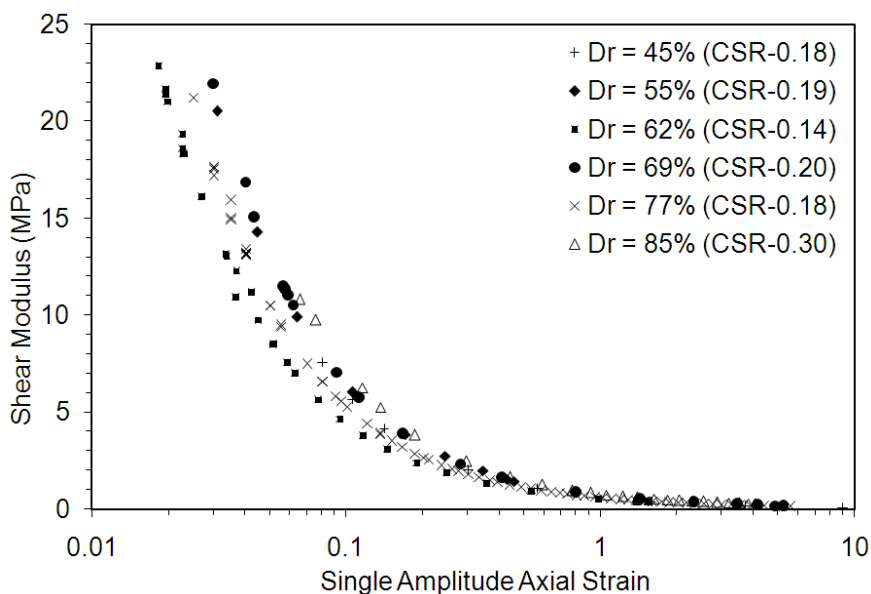


Fig. 11 Shear modulus versus single-amplitude axial strain plot for various relative densities

CONCLUSIONS

A series of undrained cyclic triaxial tests have been performed to evaluate the effects of various factors on the undrained cyclic behavior of the Sabarmati-river sand. Based on the experimental results obtained, the following conclusions have been drawn:

1. The densification of loose sand (with $D_r \leq 70\%$) increases the cyclic strength linearly. The cyclic strength increases suddenly for the dense and very dense sands (with $D_r > 70\%$) due to dilation.
2. There is an excellent correlation between CRR and normalized shear strength (as obtained from the peak and critical state) based on the CU tests. Equations (1) and (2) can be used to predict the cyclic strength from the monotonic tests. Whereas Equation (2) is useful for both the normal consolidation and dilative conditions, Equation (1) can be used for the normal consolidation conditions.
3. The pore pressure build-up in loose sands is uniform, whereas in dense sands the build-up is fast in the initial stages and decreases slightly at the later stages due to dilation.
4. Shear modulus is strain dependent and decreases with an increase in the single-amplitude strain. At low strain levels, shear modulus increases with an increase in the relative density. However, at large strains, the effect of density is erased due to the growth of anisotropy, and all samples, irrespective of their densities, have low shear moduli.

ACKNOWLEDGEMENTS

The authors thank the Ministry of Earth Sciences, Government of India for funding the research project titled "Evaluation of Liquefaction Potential Based on Cone Penetration Resistance and Shear Wave Velocity" (under Grant No. DST/23(534)/SU/2005).

REFERENCES

1. ASTM (2006a). "ASTM D4253-00: Standard Test Methods for Maximum Index Density and Unit Weight of Soils using a Vibratory Table", ASTM International, West Conshohocken, U.S.A.
2. ASTM (2006b). "ASTM D4254-00: Standard Test Methods for Minimum Index Density and Unit Weight of Soils and Calculation of Relative Density", ASTM International, West Conshohocken, U.S.A.
3. Baxter, C.D.P., Bradshaw, A.S., Green, R.A. and Wang, J. (2008). "Correlation between Cyclic Resistance and Shear Wave Velocity for Providence Silts", *Journal of Geotechnical and Geoenvironmental Engineering*, ASCE, Vol. 134, No. 1, pp. 37–46.
4. Bhandari, N. and Sharma, B.K. (2001). "Damage Pattern due to January, 2001 Bhuj Earthquake, India: Importance of Site Amplification and Interference of Shear Waves", *Proceedings of the International Conference on Seismic Hazard with Particular Reference to Bhuj Earthquake of January 26, 2001*, New Delhi, Abstract Volume, pp. 19–21.
5. BIS (2006). "IS: 2720 (Part 14)-1983—Indian Standard Methods of Test for Soils, Part 14: Determination of Density Index (Relative Density) of Cohesionless Soils (First Revision)", Bureau of Indian Standards, New Delhi.
6. Brandon, T.L., Rose, A.T. and Duncan, J.M. (2006). "Drained and Undrained Strength Interpretation for Low-Plasticity Silts", *Journal of Geotechnical and Geoenvironmental Engineering*, ASCE, Vol. 132, No. 2, pp. 250–257.
7. Dinesh, S.V. (2002). "Discrete Element Simulation of Static and Cyclic Behavior of Granular Materials", Ph.D. Dissertation, Department of Civil Engineering, Indian Institute of Science, Bangalore.
8. Finn, W.D.L. (1981). "Liquefaction Potential: Developments since 1976", *Proceedings of the First International Conference on Recent Advances in Geotechnical Earthquake Engineering and Soil Dynamics*, St. Louis, U.S.A., Vol. 2, pp. 655–681.
9. Govindaraju, L. (2005). "Liquefaction and Dynamic Properties of Sandy Soils", Ph.D. Dissertation, Department of Civil Engineering, Indian Institute of Science, Bangalore.
10. Hyodo, M., Hyde, A.F.L. and Aramaki, N. (1998). "Liquefaction of Crushable Soils", *Geotechnique*, Vol. 48, No. 4, pp. 527–543.

11. Ishihara, K., Tatsuoka, F. and Yasuda, S. (1975). "Undrained Deformation and Liquefaction of Sand under Cyclic Stresses", *Soils and Foundations*, Vol. 15, No. 1, pp. 29–44.
12. Ishihara, K. (1985). "Stability of Natural Deposits during Earthquakes", *Proceedings of the 11th International Conference on Soil Mechanics and Foundation Engineering*, San Francisco, U.S.A., Vol. 1, pp. 321–376.
13. Ishihara, K. (1993). "Liquefaction and Flow Failure during Earthquakes", *Geotechnique*, Vol. 43, No. 3, pp. 351–415.
14. Iwasaki, T. (1986). "Soil Liquefaction Studies in Japan: State-of-the-Art", *Soil Dynamics and Earthquake Engineering*, Vol. 5, No. 1, pp. 2–68.
15. JSA (2009). "JIS A 1224: 2009—Test Method for Minimum and Maximum Densities of Sands (in Japanese)", *Japanese Standards Association*, Tokyo, Japan.
16. Lee, K.L. and Seed, H.B. (1967). "Cyclic Stress Conditions Causing Liquefaction of Sands", *Journal of the Soil Mechanics and Foundation Division, Proceedings of ASCE*, Vol. 93, No. SM1, pp. 47–70.
17. Lee, K.L. and Albaisa, A. (1974). "Earthquake Induced Settlements in Saturated Sands", *Journal of the Geotechnical Engineering Division, Proceedings of ASCE*, Vol. 100, No. GT4, pp. 387–406.
18. Li, X.S., Chan, C.K. and Shen, C.K. (1988). "An Automated Triaxial Testing System" in "Advanced Triaxial Testing of Soil and Rock (edited by R.T. Donaghe, R.C. Chaney and M.L. Silver)", *Report STP 977, American Society for Testing and Materials*, Philadelphia, U.S.A.
19. Polito, C.P. and Martin II, J.R. (2001). "Effects of Nonplastic Fines on the Liquefaction Resistance of Sands", *Journal of Geotechnical and Geoenvironmental Engineering, ASCE*, Vol. 127, No. 5, pp. 408–415.
20. Ravishankar, B.V. (2006). "Cyclic and Monotonic Undrained Behaviour of Sandy Soils", *Ph.D. Dissertation, Department of Civil Engineering, Indian Institute of Science, Bangalore*.
21. Seed, H.B. (1979). "Soil Liquefaction and Cyclic Mobility Evaluation for Level Ground during Earthquakes", *Journal of the Geotechnical Engineering Division, Proceedings of ASCE*, Vol. 105, No. GT2, pp. 201–255.
22. Tatsuoka, F., Ochi, K., Fujii, S. and Okamoto, M. (1986). "Cyclic Undrained Triaxial and Torsional Shear Strength of Sands for Different Sample Preparation Methods", *Soils and Foundations*, Vol. 26, No. 3, pp. 23–41.
23. Wang, J.N. and Kavazanjian Jr., E. (1989). "Pore Pressure Development during Non-uniform Cyclic Loading", *Soils and Foundations*, Vol. 29, No. 2, pp. 1–14.
24. Wong, R.T., Seed, H.B. and Chan, C.K. (1975). "Cyclic Loading Liquefaction of Gravelly Soils", *Journal of the Geotechnical Engineering Division, Proceedings of ASCE*, Vol. 101, No. GT6, pp. 571–583.
25. Wood, F.M., Yamamuro, J.A. and Lade, P.V. (2008). "Effect of Depositional Method on the Undrained Response of Silty Sand", *Canadian Geotechnical Journal*, Vol. 45, No. 11, pp. 1525–1537.